Available online at www.sciencedirect.com
SCIENCE DIRECT®
Carbon 42 (2004) 1723–1729
CARBON
www.elsevier.com/locate/carbon

KOH activation of carbon nanofibers

Seong-Ho Yoon *, Seongyop Lim *, Yan Song, Yasunori Ota, Wenming Qiao, Atsushi Tanaka, Isao Mochida

Institute for Materials Chemistry and Engineering, Kyushu University, 6-1 Kasugakoen, Kasuga, Fukuoka 816-8580, Japan

Received 4 November 2003; accepted 1 March 2004
Available online 15 April 2004

Abstract

Catalytically grown carbon nanofiber (CNF) was activated with KOH to attain a high surface area with porous structure. The structural change of CNFs through KOH activation was investigated by using SEM, TEM and XRD. KOH activation was found to be effective to develop particular pore sizes on the CNF surface, increasing the surface area of CNF. The increase of surface area in KOH activation of CNF is first ascribed to local broadening of graphene interstices or local burn-off of graphenes, which limit the surface area increase of CNF with the fiber structure maintained. The activation under severe conditions caused to destroy the fiber structure of CNF. Activated CNFs were applied as an electrode for electrical double layer capacitors to be compared to active carbon fibers in terms of the surface properties.

Keywords: A. Carbon filaments, Catalytically grown carbon; B. Activation; C. Electron microscopy; D. Electrochemical properties

1. Introduction

Carbon nanofiber (CNF) is recognized as one of very promising materials based on its nano-structure and particular properties, being expected in various applications such as catalysts or catalyst supports, selective adsorption agents, and energy storage devices such as lithium ion second battery or electric double layer capacitor (EDLC) [1–5].

In recent development and studies of nano-sized materials including CNF, electron microscopy such as scanning electron microscopy (SEM), transmission electron microscopy (TEM) and scanning tunneling microscopy (STM), is an important technique to elucidate their detailed microstructure and various structural changes by chemical and physical modification.

Chemical activation with alkali compounds such as KOH and NaOH is a well-known method to activate carbon materials with a high surface area, but the activation mechanism is still under discussion [6–13]. The structural studies in chemical activation of carbon have not been performed enough to understand the microstructural change because of difficulty in totally analyzing activated samples of bulk sizes under TEM.

CNFs show relatively lower surface area of 50–350 m^2/g, compared to activated carbons and activated carbon fibers [1]. A particular CNF with a higher surface area is expected to show better performance in wider applications. Recently, carbon nanotube (CNT) was activated by KOH and NaOH to develop the porosity in CNT for its new applications, but the increase of the surface area is limited below 1500 m^2/g [12,14].

In the present study, a herringbone-type CNF was synthesized from ethylene over a Cu–Ni catalyst, and then was activated with KOH under prescribed conditions. This study focused on the structural changes of CNF according to the increase of surface area through KOH activation. Morphology and structure of activated CNFs were closely observed under SEM and TEM. Crystallographic parameters of activated CNFs were also examined with X-ray diffraction (XRD) in order to understand the structural changes. Electric double layer capacitance (EDLC) test was performed to examine the surface properties of activated CNFs comparing to conventional carbon fibers.

* Corresponding authors. Tel.: +81-92-5837797; fax: +81-92-5837798.
E-mail addresses: yoon@cm.kyushu-u.ac.jp (S.-H. Yoon), lim9@asem.kyushu-u.ac.jp (S. Lim).

0008-6223/$ - see front matter © 2004 Elsevier Ltd. All rights reserved.
doi:10.1016/j.carbon.2004.03.006

2. Experimental

2.1. Chemicals

Reagent grade copper nitrate [$Cu(NO_3)_3 \cdot 3H_2O$], nickel nitrate [$Ni(NO_3)_3 \cdot 6H_2O$], ammonium bicarbonate (NH_4HCO_3), and potassium hydroxide (KOH) were obtained from Wako Inc. (Japan). Gases of hydrogen (>99.9999%), ethylene (99.9%), and He (>99.9999%) were obtained from Asahi Sanso Inc. (Japan).

2.2. Preparation and activation of CNFs

Copper–nickel catalyst was prepared by the precipitation of copper and nickel carbonates from an aqueous solution of corresponding nitrate by using ammonium bicarbonate as described in detail in Ref. [15].

The apparatus used for the preparation of CNF consists of a horizontal quartz reactor tube with a conventional horizontal furnace. Cu–Ni catalyst powder (50 mg) was placed in an alumina boat at the center of the reactor tube. After reduction in a 20% (v/v) H_2/He mixture at 600 °C for 2 h, helium was flushed for 30 min before introduction of C_2H_4/H_2 mixture over the catalyst. The total flow rate was 200 ml/min through the whole process. The total amount of carbon deposited during the time on stream was determined gravimetrically after cooling the product to ambient temperature.

In KOH activation, CNF as prepared with addition of KOH was placed on a Ni-pan in a vertical type furnace of stainless steel. The ratio of KOH and CNFs is fixed in 4:1 (g/g). Activation conditions were 500–1000 °C for 1–5 h at the heating rate of 5 °C/min under argon flow of 100 ml/min. The activated product was washed using distilled water, filtered and then dried at 105 °C.

2.3. Characterizations

2.3.1. Surface area of CNFs and their activated forms

Nitrogen adsorption isotherms of CNF and its activated forms were measured with Sorptomatic 1990 adsorption analyzer (FISONS Instruments) at liquid nitrogen temperature. All samples were degassed at 150 °C for 2 h prior to the measurements. The specific surface area was calculated in the relative pressure interval of 0.05–0.35 using BET (Brunauer–Emmett–Teller) method. Pore size and distribution were calculated by the BJH method from desorption curves [16].

2.3.2. X-ray diffraction (XRD) of CNF and its activated form

The crystallographic data were collected with an X-ray diffractometer (Rigaku, Cu Kα target) and the crystallographic parameter (d_{002}) was calculated according to the JSPS procedure [17]. A powdered sample was mixed with the standard silicon (200 meshes, 99.99%) at the ratio of sample to silicon 9:1 (w/w) prior to the analysis.

2.3.3. Electron microscopy of CNFs and their activated forms

The structure of CNFs as prepared and activated was examined using scanning electron microscope (JSM-6320F, JEOL) and a high resolution transmission electron microscope (JEM-2010F, JEOL).

2.3.4. Electrical double layer capacitance of CNFs and their activated forms

The capacitance was measured according to two-electrode method. The test cell consisted of a pair of electrodes and immersed in 1 M Et_4NBF_4/PC. The test cell was charged to 2.7 V at a constant current, and then discharged at a constant current (2 mA/cm^2) to 0 V. The capacitance of activated CNF was calculated according to Ref. [18].

3. Results

3.1. Preparation of CNF

CNF in this study was synthesized over a Cu–Ni (2:8) catalyst from ethylene and hydrogen (4:1) mixture at 580 °C. CNF was obtained in a high yield of 174 g per 1 g catalyst for 1 h reaction. Several properties of CNF as prepared were listed in Table 1.

3.2. KOH activation of CNF

Fig. 1 shows the effects of activation temperature on the yield and surface area of CNF-1 in KOH activation (activation time is 1 h). The surface area of CNF-1 started to increase by activation at higher than 600 °C with corresponding decrease of carbon yields. KOH activation of CNF-1 at 850 °C resulted in 491 m^2/g surface area and 74% (w/w) yield (26% burnt-off). The surface area and the carbon yield of CNFs changed remarkably at 1000 °C (1212 m^2/g surface area and 45% yield).

Table 1
Preparation parameters and properties of CNFs

	Synthesis temperature (°C)	CNF yield[a]	Diameter (nm)	Surface area (m^2/g)	Pore volume (cm^3/g)	d_{002} (nm)	Lc(002) (nm)
CNF-1	600	174	80–350	143	0.108	0.3416	4.57

[a] The yield (g CNF/g catalyst) was gravimetrically calculated as the weight of CNF produced per the weight of catalyst after 1 h reaction.

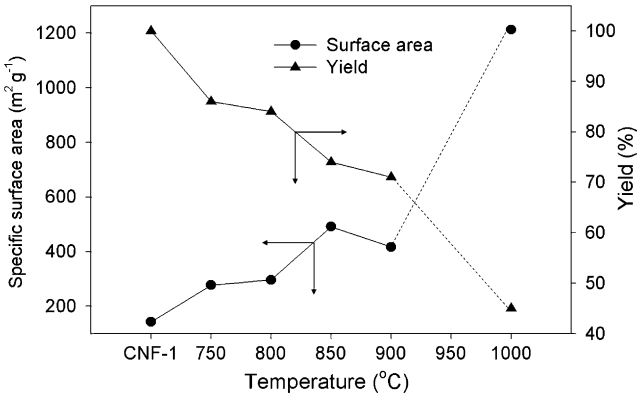

Fig. 1. Specific surface area of activated CNF-1s and activation yield depending on activation temperatures.

Fig. 2 shows the effects of activation time on surface area after KOH activation (activation temperatures were 800 and 850 °C). KOH activation of CNF-1 at 800 and 850 °C for 3 h provided the maximum surface areas of 439 and 587 m^2/g, respectively, which are 3–4 times higher than as-prepared CNF-1.

3.3. Adsorption isotherm and pore distribution

Fig. 3a shows nitrogen sorption isotherms of CNF-1 and several activated samples. Differing from intact CNF-1, the isotherms of CNFs activated with KOH exhibit hysteresis loops, suggesting mesoporous features. In Fig. 3b, the pore size distributions calculated from desorption branch by BJH method show particular pore sizes developing around hydraulic radius 1.8 nm as the surface area increases by KOH activation. CNF activated at 1000 °C (showing a high surface area of 1212 m^2/g) exhibits a complex pore system consisting of not only the particular pores around 1.8 nm but also a large amount of other size pores in a wide range of 1–10 nm.

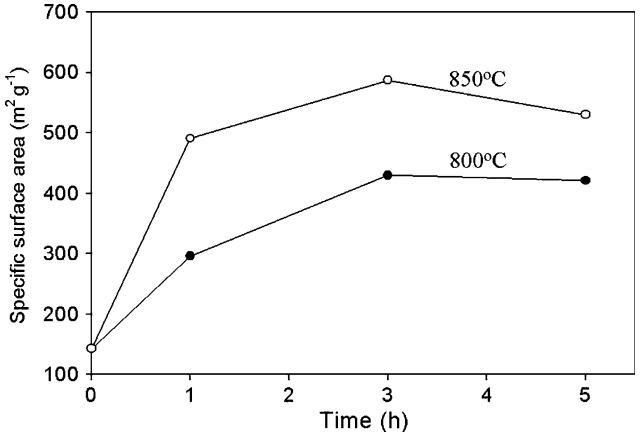

Fig. 2. Effect of the activation time on the surface area of activated CNF-1.

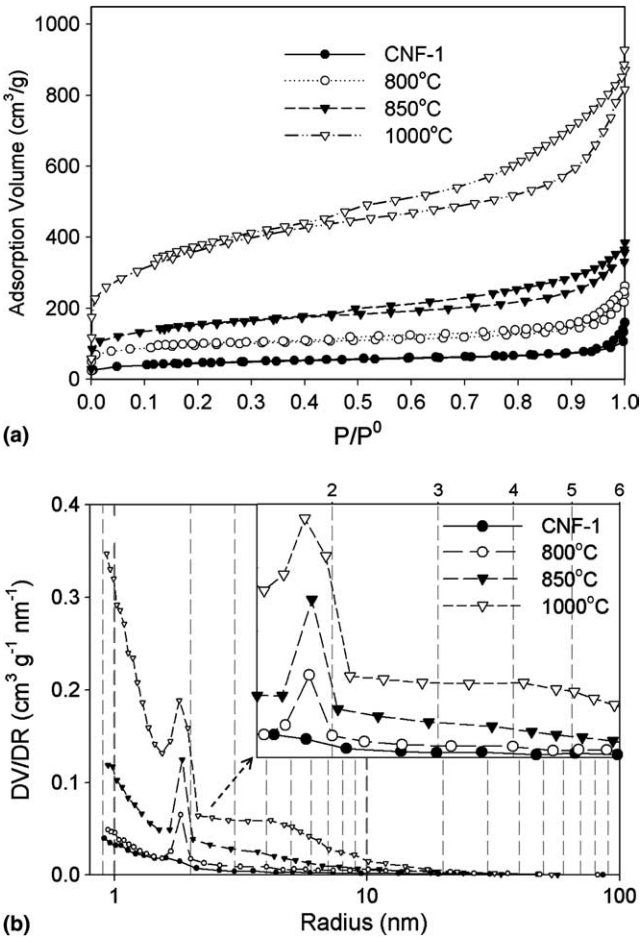

Fig. 3. Nitrogen adsorption isotherms (a) and pore size distribution (b) of CNF-1 as prepared and activated with KOH.

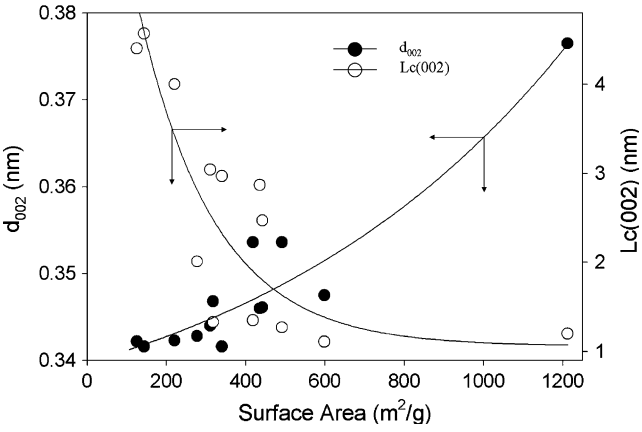

Fig. 4. The d_{002} (solid circles) and Lc(0 0 2) (open circles) of CNF-1 as prepared and activated with KOH obtained through X-ray diffraction.

3.4. XRD properties of CNFs as prepared and activated with KOH

The average (0 0 2) interlayer spacing (d_{002}) and the average stacking height of carbon (0 0 2) planes (Lc(0 0 2)) of CNFs as prepared and activated in this study were

analyzed with powdered X-ray diffraction, being plotted versus specific surface areas as shown in Fig. 4. In CNFs with less than 400 m^2/g surface areas, the d_{002} showed just a little change, whereas the Lc(0 0 2) decreased sharply from 4.6 nm to about 1.0 nm. In CNFs with higher surface areas than 400 m^2/g, the d_{002} increased with no change in Lc(0 0 2) as the surface area increased.

3.5. Morphology and structure of CNFs as prepared and activated with KOH

Fig. 5 shows SEM pictures of CNF-1 and its activated forms. In Fig. 5a–c, CNFs as prepared and activated with KOH maintain the fiber form, and it is difficult to find any change of overall diameter and structure of CNF-1 before (see Fig. 5a) and after KOH activation (see Fig. 5b and c) under SEM, although a large amount of carbon was consumed (Fig. 1). In SEM images of high magnification, any difference was hardly found in the surface of CNF-1 before (see Fig. 5e) and after KOH activation (see Fig. 5f and g). However, the fibrous shape of the sample with a high surface area of 1212 m^2/g was wholly collapsed to become other type bulk structure (see Fig. 5d), although a minority of fibers remained to be aggregated as shown in Fig. 5h.

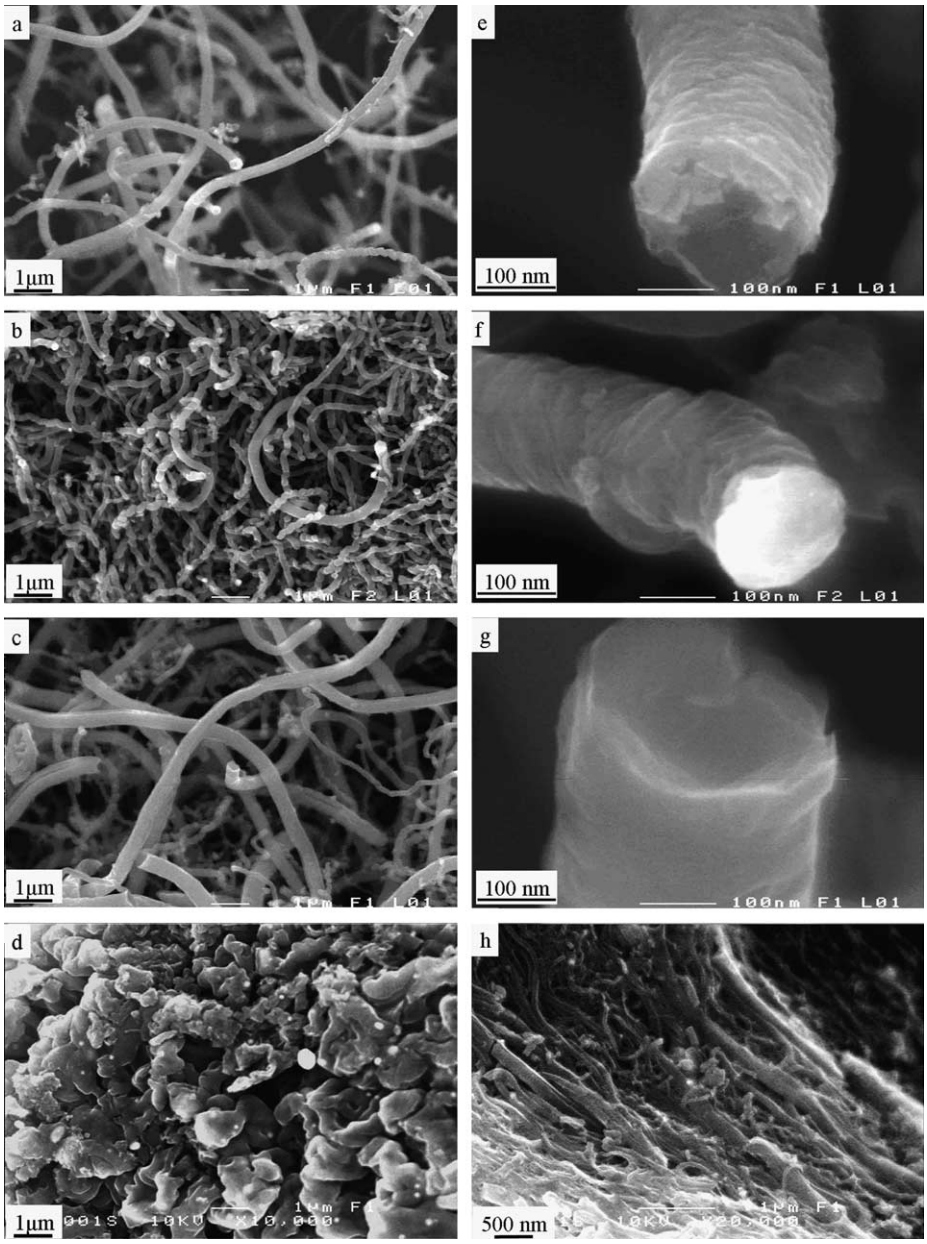

Fig. 5. SEM images of CNF-1 as prepared (a, e); activated at 850 °C for 1 h (b, f); activated at 850 °C for 3 h (c, g); and activated at 1000 °C for 1 h (d, h).

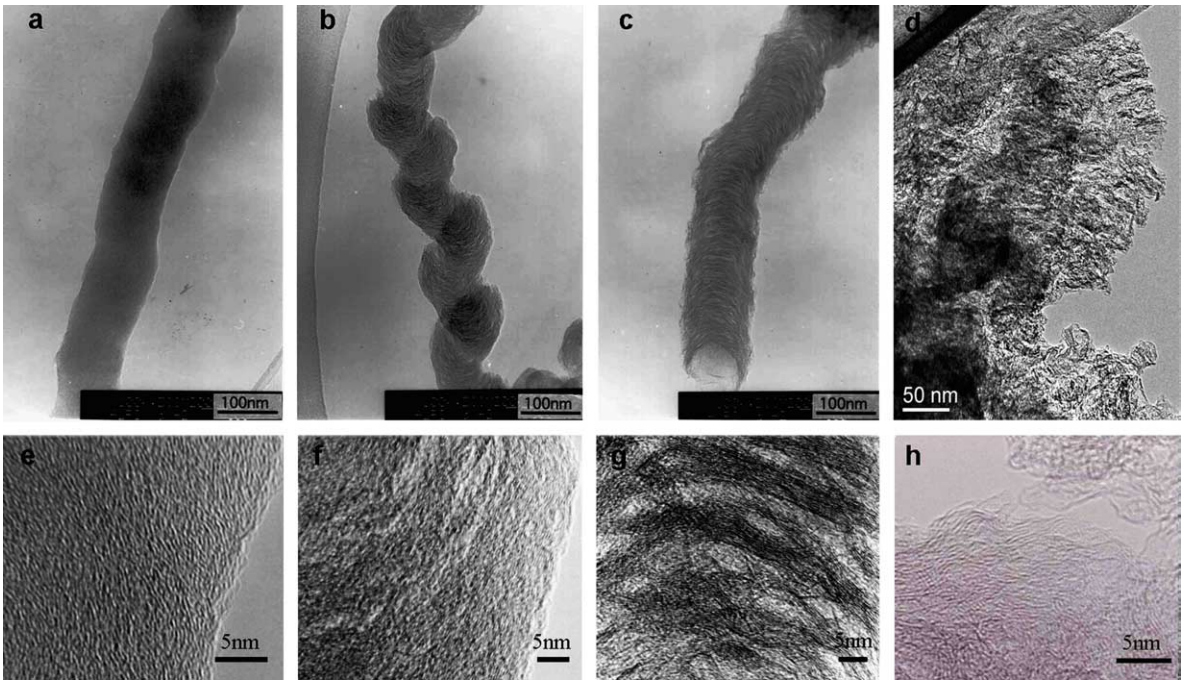

Fig. 6. TEM images of CNF-1 as prepared (a, e); activated at 850 °C for 1 h (b, f); activated at 850 °C for 3 h (c, g); and activated at 1000 °C for 1 h (d, h).

Under TEM, CNF-1 as prepared exhibits relatively thick diameters of average 150 nm with herringbone-type alignment in which the graphenes are angled to the fiber axis as shown in Fig. 6a and e. Activation caused a significant structural change, where particular parts of graphenes were consumed at a constant interval in activated CNF-1 which looks like a ladder (Fig. 6b, c, f, and g). In Fig. 6d and h, fibers were found to be perfectly destroyed in some parts and probably rearranged to form non-fibrous bulky grains as observed in conventional activated carbons.

3.6. Capacitance of activated CNFs

The capacitance of CNF-1 as prepared was around 7 F/g as shown in Fig. 7. The capacitance of activated CNF-1 increased as the surface area of activated CNF-1 increased. However, the capacitance was found to show no further increase when the fiber structure collapsed despite its high surface area. Compared to mesophase pitch-based or isotropic ACFs activated with steam or KOH, the activated CNFs showed a high capacitance with their relatively small surface area.

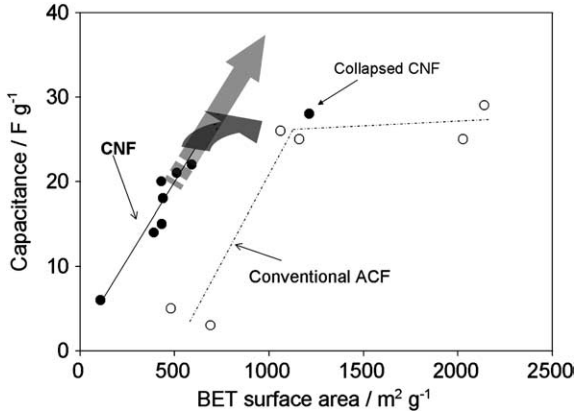

Fig. 7. Capacitance of CNFs comparing to conventional ACFs (steam and KOH activation).

4. Discussion

4.1. Structural change in KOH activation of CNF

It is well known that preparation of carbon materials by KOH activation generally leads to a very high surface area of even more than 2000 m^2/g. Such a high surface area is ascribed to partial gasification and expansion of the interlayer spacing between graphenes through simultaneous intercalation and deintercalation [6,10–13]. It has been reported to be difficult to activate carbon materials with high graphitization degree or develop its micro-porosity even by the chemical activation [19]. In this study, KOH activation was far still effective to develop the porosity of CNF with its original fibrous form and diameter sustained. Activated CNF-1 showed a ladder-like structure in the fibrous form, where the interspacing of (0 0 2) planes increased not between all of graphenes but at an interval of some of nano-sized units probably due to selective consumption of graphenes.

Such a locally-broadened interspacing appears to provide the porosity and surface area, especially with mesoporous characteristics. However, a high surface area of more than 1000 m^2/g by severe activation appears to correspond to destruction of the fibrous form and graphitic layered structure.

CNF-1 maintained its diameter until the yield of KOH activation was around 70% (w/w). From XRD results, the average stacking height of (0 0 2) plane was found to decrease according to increase of surface area with little change in the (0 0 2) plane interspacing in the initial stage of KOH activation, which suggests that selective consumption of graphenes in certain parts occurs first. Such a structural change corresponds to the ladder-like structure of activated CNF-1 with its fiber shape maintained. Severe activation causes broadening and collapsing of overall (0 0 2) plane interspacing to destroy and rearrange the fiber structure. From the results, a schematic model (see Fig. 8) is suggested for the KOH activation of CNF as following:

(1) Selective gasification of graphenes by components from KOH.
(2) Formation of ladder-like structure by local removal or broadening of graphene layers (fibrous form was maintained).
(3) Collapse and rearrangement of graphene layers (fibrous form was destroyed).

Recently the present authors found a nano-sized rod-type unit in structural hierarchy of CNF by combining the observation under SEM, TEM and STM, and proposed a structure concept of CNF being constructed by such a nano-sized unit, which is approximately 2.5 nm in the average width (8–10 carbon hexagon layers) and variable in the length depending on the fiber dimension [20,21]. Such a structural concept also may explain KOH activation of CNF. KOH activation broadens first the interstices between the structural units first, and further reaction causes to destroy overall fiber structure to be rearranged into accumulative amorphous carbons as illustrated in Fig. 8.

4.2. Electric double layered capacitance (EDLC) of activated CNFs

CNF is characterized by the graphite-like structure, where the stacking of nano-sized graphenes is quite uniform along the whole fiber axis, differing from activated carbon fibers. CNFs activated with KOH were found to have particular pores developing around 1.8 nm hydraulic radii. Also, as the activation progressed, the mesoporous characteristics appeared in activated CNFs. As results of EDLC test, activated CNF-1s in spite of relatively low surface areas showed higher capacitance than ordinary activated carbon fibers or cokes with similar surface areas. However, the collapsed CNF by KOH activation did not follow the tendency of activated CNFs which sustained its fiber structure. In the collapsed CNF, various pores developed probably due to complex structure formed by decomposition and rearrangement of CNF graphenes, although the amount of the particular pores in fibrous activated CNFs also increased. If other factors affecting the capacitance are excluded, the optimum pore structure and dimension appear to exist. However, the structure and surface of CNF are basically different from active carbon or carbon fibers, and hence more detailed examination should be performed.

5. Conclusion

In this study, we investigated the structure change of CNF through KOH activation on advantage of facile observation of the microstructure under TEM. Development of particular pores in CNFs by KOH activation

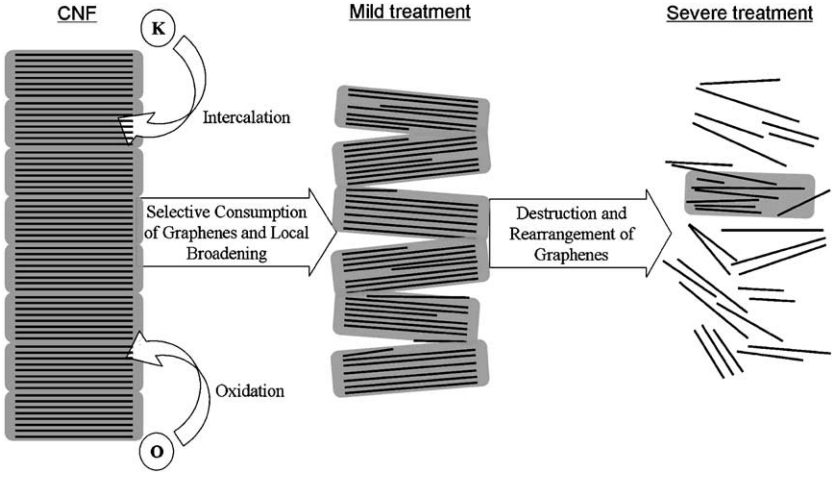

Fig. 8. Schematic suggestion of KOH activation of CNF.

corresponds to the particular structure change that is selective consumption of graphenes and local broadening of the interspacing between structure units consisting of several graphenes. Consequently, a ladder-like structure was formed and severe activation caused to destroy the fiber structure, providing other-type porous carbon materials. In spite of a little information on the chemistry of KOH activation, the structural study is expected to provide significant insight on the structure itself and the formation of pores contributing to the surface area of carbon materials.

References

[1] Rodriguez NM. A review of catalytically grown carbon nanofibers. J Mater Res 1993;8(12):3233–50.

[2] Dai H, Wong EW, Lu YZ, Fan S, Lieber CM. Synthesis and characterization of carbide nanorods. Nature 1995;375:769–72.

[3] Matsumoto M, Hashimoto T, Uchiyama Y, Murata K, Goto S. Use of modified carbon whiskers as an electrode in coulometric cells. Carbon 1993;31(6):1003–4.

[4] Frackowiak E, Gautier S, Gaucher H, Bonnamy S, Beguin F. Electrochemical storage of lithium multiwalled carbon nanotubes. Carbon 1999;37:61–9.

[5] Ebbesen TW, Ajayan PM. Large-scale synthesis of carbon nanotubes. Nature 1992;358:220–1.

[6] Marsh H, Yan DS, O'Grady TM, Wennerberg A. Formation of active carbons from cokes using potassium hydroxide. Carbon 1984;22(6):603–11.

[7] Ehrburger P, Addoun A, Addoun F, Donnet JB. Carbonization of coals in the presence of alkaline hydroxides and carbonates: formation of activated carbons. Fuel 1986;65:1447–9.

[8] Otawa T, Nojima Y, Miyazaki T. Development of KOH activated high surface area carbon and its application to drinking water purification. Carbon 1997;35(9):1315–9.

[9] Lozano-Castelló D, Lillo-Ródenas MA, Cazorla-Amorós D, Linares-Solano A. Preparation of activated carbons from Spanish anthracite. I. Activation by KOH. Carbon 2001;39(5):741–9.

[10] Ahmadpour A, Do DD. The preparation of active carbons from coal by chemical and physical activation. Carbon 1996;34(4):471–9.

[11] Yoshizawa N, Maruyama K, Yamada Y, Ishikawa E, Kobayashi M, Toda Y, et al. XRD evaluation of KOH activation process and influence of coal rank. Fuel 2002;81(13):1717–22.

[12] Raymundo-Pinero E, Azais P, Cazorla-Amoros D, Linares-Solano, Szostak K. Study of the activation mechanism of carbon nanotubes by KOH and NaOH. In: Extended Abstracts, Carbon 2003: International Conference, Oviedo, Spain, July 6–10. Spanish Carbon Group, 2003. p. 55.

[13] Lillo-Rodenas MA, Cazorla-Amoros D, Linares-Solano A. Understanding chemical reactions between carbons and NaOH and KOH—an insight into the chemical activation mechanism. Carbon 2003;41(2):267–75.

[14] Raymundo-Piñero E, Cazorla-Amorós D, Linares-Solano A, Delpeux S, Frackowiak E, Szostak K, et al. High surface area carbon nanotubes prepared by chemical activation. Carbon 2002;40(9):1614–7.

[15] Best RJ, Russell WW. Nickel, copper and some of their alloys as catalysts for ethylene hydrogenation. J Am Chem Soc 1954;76:838–42.

[16] Barrett EP, Joyner LG, Halenda PP. The determination of pore volume and area distributions in porous substances. 1. computations from nitrogen isotherms. J Am Chem Soc 1951;73(1):373–80.

[17] Japan Society for the Promotion of Science (117th committee). On the measurement of lattice parameters and unit cell dimension of artificial graphite. Tanso 1963;36:25–34 [in Japanese].

[18] Qiao WM, Korai Y, Mochida I, Hori Y, Maeda T. Preparation of an activated carbon artifact: oxidative modification of coconut shell-based carbon to improve the strength. Carbon 2002;40(3):351–8.

[19] Macia-Agullo JA, Moore BC, Cazorla-Amoros D, Linares-Solano A. Chemical activation by KOH and NaOH of carbon materials with different crystallinity. In: Extended Abstracts, Carbon 2003: International Conference, Oviedo, Spain, July 6–10. Spanish Carbon Group, 2003. p. 197.

[20] Yoon SH, Tanaka A, Lim SY, Korai Y, Mochida I, Ahn B, Yokogawa K, Park CW. 3-Dimensional Structure of carbon nanofiber: carbon nano rod. In: Extended Abstracts, Carbon 2003: International Conference, Oviedo, Spain, July 6–10. Spanish Carbon Group, 2003. p. 76.

[21] Lim S, Yoon S-H, Mochida I, Chi J-H. Surface modification of carbon nanofiber with high degree of graphitization. J Phys Chem B 2004;108(5):1533–6.